

# NUCLEAR MATTER MEAN FIELD WITH EXTENDED NJL MODEL

**Steven A. Moszkowski**  
*UCLA, Los Angeles, CA 90095, USA*

**Constança Providência, João da Providência and João M. Moreira**  
*University of Coimbra, P-3000 Coimbra, Portugal*

October 25, 2018

## Abstract

An extended version of the Nambu-Jona-Lasinio (NJL) model is applied to describe both nuclear matter and surface properties of finite nuclei. Several parameter sets are discussed and a comparison of the saturation properties and equation of state (EOS) with the NL3 parametrization of the non-linear Walecka model is made. The properties of asymmetric matter are discussed.

## 1 Introduction

Strong interaction dynamics of mesons and baryons is believed to be described by QCD. This theory exhibits a non perturbative behaviour at low energies, a circumstance which renders the analytic study of the theory rather difficult. The NJL model is a popular substitute which has in common with QCD important symmetries of the quark-flavour dynamics. This model has been very successful in the description of the meson sector. The question arises whether the model also allows for inhomogeneous solutions at non-zero density which are of interest for the description of hadronic matter.

The NJL model [1] was originally developed for the purpose of understanding hadron physics. In this model, hadron masses are generated by spontaneous symmetry breaking of the vacuum. In the modern form of the NJL model, we start with essentially massless quarks interacting via zero range interactions, but with a cutoff in momentum space [2, 3, 4]. NJL is thus only an effective theory, in which form factors and other finite range effects have been ignored, and it does not take into account quark confinement. However, it may work quite well in the region of interest in nuclear physics, i.e. for excitations less than the scalar meson mass.

The paper has been organized as follows: It is shown that with the generalization of the NJL model for nucleons, referred to as the Extended NJL (ENJL) model, it is possible to get a reasonable nuclear equation of state and behaviour of the effective mass. Then we list some numerical results, concerning both nuclear matter and quark matter. It is found that the performance of the ENJL model is almost perfect as far as bulk static properties, such as saturation and binding energy of nuclear matter, or the effective mass of nucleons, are concerned. However, the model fails when we wish to deal with dynamical properties, since it leads to scalar excitations with the unacceptable mass of twice the nucleon mass,

or to a poor description of the nuclear surface. In order to overcome these drawbacks, the ENJL model is replaced by a chiral invariant model of nucleons interacting through the exchange of  $\sigma$ ,  $\vec{\pi}$  and  $\omega$  fields, which we call extended chiral sigma (ECS) model. For the description of bulk static properties, the ECS model is almost equivalent to the ENJL model. In these models, the nucleons are regarded as composite particles. The composite nature of the particles reflects itself in the fact that the coupling depends on the local density. The surface properties of finite nuclei are calculated within the ECS model. Some remarks concerning the connection of the ENJL and ECS models to other relativistic chiral models [5, 6] are presented. Then, some properties of asymmetric nuclear matter are discussed and some brief conclusions are drawn. Next, we discuss a two dimensional version of the NJL model for which some simple analytic results can be obtained. This is followed by a comparison of our model with several other models, including the quark meson coupling model and versions of relativistic mean field models. Preliminary results of the present work have been presented in [9].

## 2 NJL model

### 2.1 Original NJL Model

The NJL model [3] is defined by the Lagrangian density

$$\mathcal{L} = \bar{\psi}(i\gamma^\mu\partial_\mu)\psi + G[(\bar{\psi}\psi)^2 + (\bar{\psi}i\gamma_5\vec{\tau}\psi)^2]. \quad (1)$$

A regularizing momentum cut-off  $\Lambda$  is part of the model. The Lagrangian is equivalent to the Hamiltonian

$$\mathcal{H}_{NJL} = \sum_{k=1}^N \vec{p}_k \cdot \vec{\alpha}_k + G \sum_{k,l=1}^N \delta(\vec{r}_k - \vec{r}_l) \beta_k \beta_l (1 - \gamma_k^5 \gamma_l^5 \vec{\tau}_k \cdot \vec{\tau}_l). \quad (2)$$

The vacuum is described by a Slater Determinant  $|\Phi_0\rangle$  constructed from plane waves which are negative energy eigenfunctions of the single particle Hamiltonian  $h = \vec{p} \cdot \vec{\alpha} + \beta m$ . The ‘‘constituent mass’’  $m$  is a variational parameter.

If moreover positive energy eigenfunctions with momentum  $\vec{p}$  satisfying  $|\vec{p}| < p_F$  are occupied, so that  $p_F$  is the Fermi momentum, the energy expectation value  $E = \langle \Phi_0 | \mathcal{H}_{NJL} | \Phi_0 \rangle$  is given by

$$E = -\nu \sum_{p_F \leq |\vec{p}| \leq \Lambda} \frac{p^2}{\sqrt{m^2 + p^2}} - m^2 G \nu^2 \left[ \sum_{p_F \leq |\vec{p}| \leq \Lambda} \frac{1}{\sqrt{m^2 + p^2}} \right]^2. \quad (3)$$

For quark matter, the degeneracy is  $\nu = 2N_c N_f$  and  $\Lambda$  is such that  $m = 313$  MeV is the constituent quark mass in the vacuum. The gap equation, which determines  $m$ , reads,

$$2G\nu \sum_{p_F \leq |\vec{p}| \leq \Lambda} \frac{1}{\sqrt{m^2 + p^2}} = 1. \quad (4)$$

## 2.2 Nuclear Matter vs Quark Matter Cutoff

It is well known that the NJL model does not contain a mechanism for quark confinement. Thus the clustering of quarks into nucleons is not accounted for in this model. In this paper, quark clustering is put in by hand. The way it is done here is that we treat the nucleons as the elementary particles, but take quark structure into account in the interactions. We will find it convenient to define dimensionless integrals  $I_n$  by:

$$\int_0^x \frac{2p^2}{(1+p^2)^{n-\frac{1}{2}}} dp = I_n(x). \quad (5)$$

According to the NJL model, the volume integral of the  $NN$  interaction is given by

$$\tilde{V}_s = -4 \frac{\pi^2}{I_2(\frac{\Lambda N_c}{M_0})} N_c \mu c^2 \left(\frac{\hbar}{\mu c}\right)^3 = -8.99 N_c^3 M_0 c^2 \left(\frac{\hbar}{M_0 c}\right)^3. \quad (6)$$

Here  $N_c$  is the number of colors, and  $M_0$  is the free nucleon mass. For quark matter,  $N_c = 3$ . The scalar ( $\sigma$ ) meson mass is:

$$\mu = m_s = \frac{2M_0}{N_c}. \quad (7)$$

Let us now try to get the same  $NN$  volume integral with a single color. This can be accomplished by using a lower value of the cutoff, denoted here by  $\Lambda'$ . Further, from here on, we will often express all masses in units of the free nucleon mass  $M_0$ . Also, we will set  $\hbar$  and  $c$  equal to 1. We find that:

$$I_2(\Lambda') = \frac{I_2(\Lambda N_c)}{N_c^3}. \quad (8)$$

An alternative way of taking quark clustering into account is by fixing  $\Lambda'$  so that the free nucleon mass in vacuum,  $M_0$  is preserved. Actually, such a prescription has been adopted in some of the calculations which are reported in Section 4 of this paper. However, the value of  $\Lambda'$  so obtained is in a very reasonable qualitative agreement with the one determined by eq. (8).

## 2.3 Extended NJL Model

The NJL model can be extended [7, 8, 9, 10] to yield reasonable saturation properties of nuclear matter, the field  $\psi$  being then the nucleon field. In Ref. [8], the nucleon is constructed as a 3-quark bound state, this quark substructure giving rise to a mechanism for saturation of nuclear matter which plays the same role as the 8-fermion term in our ENJL model. Such substructure may therefore be regarded to provide a microscopic basis for our phenomenological approach. An effective density dependent coupling constant is obtained if the following extended NJL (ENJL) Lagrangian density, which actually pushes chiral symmetry restoration to higher densities, is considered,

$$\begin{aligned} \mathcal{L} &= \bar{\psi}(i\gamma^\mu \partial_\mu)\psi + G_s[(\bar{\psi}\psi)^2 + (\bar{\psi}i\gamma_5\vec{\tau}\psi)^2] - G_v(\bar{\psi}\gamma^\mu\psi)^2 \\ &- G_{sv}[(\bar{\psi}\psi)^2 + (\bar{\psi}i\gamma_5\vec{\tau}\psi)^2](\bar{\psi}\gamma^\mu\psi)^2. \end{aligned} \quad (9)$$

		Coupling constants, etc.	
Quantity	EOSI	Quantity	EOSI
$G_s(\text{fm}^2)$	3.880	$M_0$ (MeV)	939
$G_v(\text{fm}^2)$	3.952	$\Lambda$ (MeV)	418.9
$G_{sv}(\text{fm}^8)$	-4.901	$I_1$	0.0560
$G_\rho(\text{fm}^2)$	2.794	$I_2$	0.0502
$c_v$	0.913	$\rho/\rho_0$ ( $M = 0$ )	3.0
$c_{sv}$	0.427	$E_{Bq} = E_{BN}$ (MeV)	111
$\tilde{V}_S$	-1705.4	$\rho/\rho_0$ ( $E_{Bq} = E_{BN}$ )	4.3

Table 1: The coupling constants and properties for our preferred equation of state

For nuclear matter  $\psi$  is the nucleon field, the degeneracy is  $\nu = 2N_f$  and  $\Lambda$  is such that  $M = 939$  MeV is the nucleon mass in the vacuum, determined variationally, as explained below. A different extension which also leads to nuclear saturation has been made [11, 12], This involves the fourth power of the scalar density. Another alternative way of extending the NJL model was studied by Rezaeian and Pirner [13]. Here the nucleon is considered to be a composite particle, a bound state of a quark and a diquark. The term in  $G_v$  is supposed to simulate a chiral invariant short range repulsion between nucleons connected, possibly, with the chromomagnetic interaction between quarks. The term in  $G_{sv}$  accounts for the density dependence of the scalar coupling between nucleons which is a manifestation of the composite nature of these particles and is equivalent to allowing the coupling constant  $G$  in the original NJL model to depend on  $\rho$  in such a way that  $G$  becomes replaced by  $G_s(\rho) = G_s(1 - \frac{G_{sv}}{G_s}\rho^2)$ . It is found that the magnitude of the  $\sigma$  field decreases as the hadronic density increases, in accordance with the corresponding tendency for chiral symmetry restoration. This mechanism has a similar effect, for saturation, as the analogous one proposed by Guichon [14], according to which confinement is affected by an increase of the density in such a way as to become gradually less effective, which amounts to an increasing repulsion. For nuclear matter, the NJL model leads to binding but the binding energy per particle does not have a minimum except at a rather high density where the nucleon mass is small or vanishing. Thus the pure NJL model does not give a proper equation of state. The introduction of the  $G_{sv}$  coupling term is required to correct this. On the other hand, for quark matter we set  $G_v = G_{sv} = 0$ . For quark matter the energy per particle  $W$  predicted by NJL does not lead to binding and does not have a minimum except for unreasonably small values of the cutoff momentum  $\Lambda$ .

The thermodynamical potential per volume corresponding to (9) is

$$\omega(\mu) = \langle \bar{\psi}(\vec{\gamma} \cdot \vec{p})\psi \rangle - G_s \langle \bar{\psi}\psi \rangle^2 + G_v \langle \psi^\dagger\psi \rangle^2 + G_{sv} \langle \bar{\psi}\psi \rangle^2 \langle \psi^\dagger\psi \rangle^2 - \mu \langle \psi^\dagger\psi \rangle \quad (10)$$

where exchange terms have been neglected. By  $\langle \bar{\psi}\Gamma\psi \rangle$  we denote the expectation value per volume.  $\langle \bar{\psi}\Gamma\psi \rangle = \frac{1}{V} \langle \Phi_0 | \sum_k \beta_k \Gamma_k | \Phi_0 \rangle$ . The condition  $\partial\omega/\partial M = 0$  implies

$$M = -2G_s \langle \bar{\psi}\psi \rangle + 2G_{sv} \langle \bar{\psi}\psi \rangle \langle \psi^\dagger\psi \rangle^2.$$

Here  $M$  is the  $\mu$  dependent nucleon mass. To avoid a cumbersome notation, the  $\mu$  dependency is not explicitly indicated but is implicitly assumed, without danger of confusion. The free nucleon mass  $M_0$  is the value of  $M$  for  $\mu = 0$ . The condition  $\partial\omega/\partial p_F = 0$  implies

$$E_{p_F} = \mu - 2G_v \langle \psi^\dagger\psi \rangle - 2G_{sv} \langle \psi^\dagger\psi \rangle \langle \bar{\psi}\psi \rangle^2,$$

	EOSI	NL3
$E/A - M_0(\text{MeV})$	-16.12	-16.3
$\rho_0 (\text{fm}^{-3})$	0.148	0.148
$M/M_0$	0.75	0.60
$K (\text{MeV})$	295	272
$W_{surf} (\text{MeV})$	19.43	19.38
$R \text{ fm}$	5.33	5.328
$t \text{ fm}$	2.64	2.65

Table 2: Nuclear matter saturation properties and surface properties

with  $E_{p_F} = \sqrt{M^2 + p_F^2}$ . These conditions fix the values of  $p_F$ ,  $M$  for given  $\mu$ . We observe that the gap equation, which determines  $M$ , is the same as eq. (4) except for the replacement of  $G$  with  $G_s(1 - \frac{G_{sv}}{G_s}\rho^2)$ . The choice with  $G_s$  as a phenomenological parameter fixed so that nuclear matter saturation properties are reproduced, we will refer to as model I. The value of  $G_s$  is about 20% smaller than that obtained from the NJL model. On the other hand, it is also tempting to choose  $G_s$  for nuclear matter nine times bigger than the quark matter value,  $G$ . The philosophy behind the last assumption is that the NN interaction is due to the instanton interaction between quarks, predicted by QCD in the weak coupling regime. This choice of  $G_s$  defines what we will denote in the sequel as model II.

The properties of the extended NJL model are now easily computed.

### 3 Properties of nuclear matter

In Table 1, numerical results pertaining to our preferred model EOSI are presented. As input, we use the saturation properties of nuclear matter fitted empirically in Ref.[15]. The three coupling constants  $G_s, G_v$  and  $G_{sv}$  are adjusted to fit an effective mass  $M(\rho_0) = 0.75M_0$  and the saturation energy and density. Model EOSI seems to be quite realistic, since it fits well both saturation properties and the nuclear surface properties. We also compare our results with those of [16] in which a relativistic mean field theory (RMF) is used, and which describes well both stable and unstable nuclei. The RMF parametrization introduced in [16] is known as NL3. Model I gives results quite close to NL3 especially for the surface properties (see Table 2). The relation between the coupling constants  $G_s, G_v, G_{sv}$  and the parameters  $c_v, c_{sv}$ , which will be used later, is fixed as follows:

$$G_s = \frac{\pi^2}{2I_1(\Lambda') M_0^2} \quad (11)$$

$$G_v = \frac{1}{2}c_v \frac{\widetilde{V}_s}{\hbar c} = \frac{\pi^2 c_v}{2I_2(\Lambda') M_0^2} = G_s \frac{I_1(\Lambda')}{I_2(\Lambda')} c_v \quad (12)$$

$$G_{sv} = -\frac{\pi^6 c_{sv}}{2I_1(\Lambda')^2 I_2(\Lambda') M_0^8} = -G_s \frac{\pi^4 c_{sv}}{I_1(\Lambda') I_2(\Lambda') M_0^6} \quad (13)$$

Here  $M_0 = 4.76 \text{ fm}^{-1}$ . The crucial role played by clustering must be stressed. It should be pointed out that without clustering there is no real binding and that, moreover, the

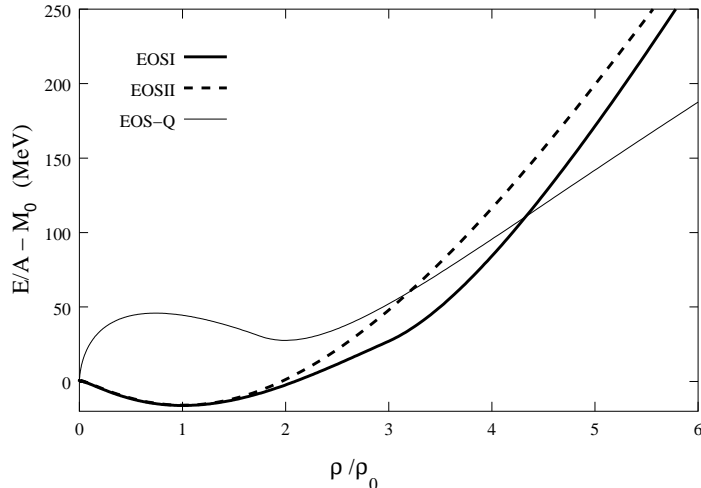


Figure 1: Energy vs density in ENJL Model for symmetric nuclear matter (EOSI and EOSII) and for quark matter (EOSI-Q)

incompressibility becomes unacceptable. In Fig. 1 we plot the binding energy for nuclear matter and quark matter (EOS-Q). For the latter case, we use a quark NJL model which differs from the nucleon NJL model (ENJL) used in the rest of this paper. At some density, the nucleon matter curve intercepts the quark matter curve, so it is clear that, at high density, quark matter prevails and may be found, for instance, in the core of neutron stars. Our experience with this problem tells us that without clustering and without the eight fermion interaction (that is, the density dependent coupling) saturation comes closely after chiral symmetry restoration, almost coinciding with it. Clustering and the eight fermion interaction places chiral symmetry restoration well after saturation.

The philosophy underlying model EOS II is to use a coupling  $G_s$  9 times bigger than  $G$  in the quark NJL model and to fit one less quantity. Thus the effective mass at saturation was left free. We have taken  $E/A = -15.8$  MeV and  $\rho_0 = 0.148$  fm $^{-3}$ , i.e.  $k_F = 0.130$  fm $^{-1}$  according to [15, 16]. Using this model, one gets quite different results for the coupling constants from EOS I, namely  $G_s = 1.746$  fm $^2$ ,  $G_v = 3.387$  fm $^2$ ,  $G_{sv} = -1.839$  fm $^8$ ,  $\Lambda = 553$  MeV. The effective mass at the saturation density turns out to be 0.89, much closer to the free nucleon mass than for model I. Also, this model leads to surface energy and thickness only about half of the empirical values. Similar results are obtained by Koch et al, ref. [7]. However, the cutoff  $\Lambda$  obtained using EOS II is not far from the one determined by eq. (8).

## 4 Surface properties

Next we will calculate nuclear surface properties which are mainly determined by the scalar meson, the meson responsible for the nuclear attraction. We have seen that the ENJL model accounts adequately for bulk static properties of hadronic matter, such as saturation and binding energy of nuclear matter, or the effective mass of nucleons. However, the model fails when we wish to deal with dynamical properties, since, as it has been shown [9, 12], it leads

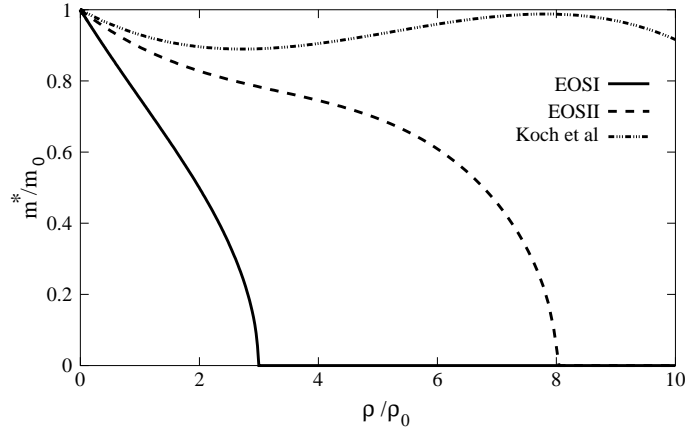


Figure 2: Effective Mass vs density in ENJL Model for models I and II and results of Koch et al. [7]

to scalar excitations with the unacceptable mass of twice the nucleon mass, and to a poor description of the nuclear surface. We keep the ENJL Lagrangian, in spite of the referred drawbacks, because it is extremely simple and transparent, clarifies the underlying physics and incorporates in the simplest possible manner the basic philosophy of our approach.

In the extended chiral sigma model, introduced in [9, 12], the nucleons and mesons are regarded as composite particles. The version used in [12] is referred to as ESM. In the present paper and in [9], a slightly different version is used which we refer to as ECS. Both models are equivalent to corresponding ENJL models, as far as ground state properties are concerned, provided exchange terms are neglected. However, there are significant differences between the models. In ESM, the coupling to the sigma meson depends on the scalar-pseudoscalar field, while in the ECS model, that coupling depends on the baryon density. Moreover, the nuclear calculations are more easily implemented in the ECS model, which is free of instability that may occur in ESM. The advantage of the ECS model over ENJL stems from the fact that it generates adequate collective properties, this being the reason that ECS can be used to study the nuclear surface.

We write formally the ECS model Lagrangian density as

$$\begin{aligned} \mathcal{L} = & \bar{\psi}(i\gamma^\mu\partial_\mu)\psi - g_s(\sigma\bar{\psi}\psi + \bar{\psi}i\gamma_5\vec{\pi}\cdot\vec{\tau}\psi)[1 + a_1(\bar{\psi}\gamma_\mu\psi)(\bar{\psi}\gamma^\mu\psi)]^{1/2} - g_v\bar{\psi}V^\mu\gamma_\mu\psi \\ & + \frac{1}{2}(\partial^\mu\sigma\partial_\mu\sigma + \partial^\mu\vec{\pi}\cdot\partial_\mu\vec{\pi}) - \frac{1}{2}m_s^2(\sigma^2 + \vec{\pi}\cdot\vec{\pi}) - \frac{1}{4}V^{\mu\nu}V_{\mu\nu} + \frac{1}{2}m_v^2V^\mu V_\mu, \end{aligned} \quad (14)$$

with

$$\frac{g_s^2}{2m_s^2} = G_s, \quad \frac{g_v^2}{2m_v^2} = G_v, \quad \frac{a_1 g_s^2}{2m_s^2} = -G_{sv}. \quad (15)$$

For comparison, the ESM Lagrangian density is given by Eq.(11) of [12], while in the linear sigma model, ref. [17], we have:

$$\begin{aligned} \mathcal{L} = & \bar{\psi}(i\gamma^\mu\partial_\mu)\psi - g_s\sigma\bar{\psi}\psi + \frac{1}{2}(\partial^\mu\sigma\partial_\mu\sigma + \partial^\mu\vec{\pi}\cdot\partial_\mu\vec{\pi}) \\ & - \frac{m_s^2}{8F_\pi^2}(\sigma^2 + \vec{\pi}\cdot\vec{\pi} - F_\pi^2)^2 \end{aligned} \quad (16)$$

Here the nucleon mass is generated by a ‘‘Mexican Hat’’ potential. If we write  $\sigma = \sigma_0 + F_\pi$  then the last term in the linear sigma model contributes  $-\frac{1}{2}m_s^2\sigma_0^2(1 + \frac{\sigma_0}{2F_\pi})^2$  to the Lagrangian. It was shown in [18] that the Dirac-sea in the linear sigma model with valence and Dirac-sea quarks but no ‘‘Mexican hat’’ provides the above effective mesonic self-interaction. The quantity  $F_\pi$  is equal to  $\sigma = M/g_s$ , when the energy is minimized w.r.t.  $\sigma$ . For zero particle density, we obtain, according to the ECS model, Eq. (14),

$$\frac{g_s^2}{2m_s^2} = \frac{9g_s^2}{8M_0^2} = G_s = \frac{\pi^2}{2I_1(\frac{\Lambda}{M_0})M_0^2},$$

which leads to

$$F_\pi(ECS) = \frac{3M_0}{2\pi} \left[ I_1\left(\frac{\Lambda}{M_0}\right) \right]^{1/2}. \quad (17)$$

This is to be compared to the pion decay constant according to the ENJL model, which, for vacuum properties such as the present one, coincides with the nucleon NJL model,

$$F_\pi(NJL) = \frac{M_0}{2\pi} \left[ I_2\left(\frac{\Lambda}{M_0}\right) \right]^{1/2}. \quad (18)$$

We observe that Eq. (18) may be obtained from Eq. (3.26)(a) of Ref. [3] upon replacing the number of colours  $N_c$  by 1 and  $m^*$  by  $M_0$ . The quantities  $I_1$  and  $I_2$  are defined in Section 2.2. The calculated pion decay constants for the ECS model (106.1 MeV) is in fairly good agreement with the empirical value of 93 MeV, but the pion decay constants for the ENJL model (33.49 MeV) is not. This was expected since the performance of the ENJL model is poor for dynamical properties.

In order to describe surface properties we must include gradient terms in the meson field [19]. Somewhat analogously to our approach, in Ref. [11] supplementary gradient terms were introduced into some kind of extended NJL model with nucleons. This is in consonance with the work [20] where an effective field theory of many-nucleon systems is obtained from the NJL type Lagrangian. In the ECS Lagrangian (14), we will keep only the gradient terms corresponding to the scalar meson, the philosophy behind this approximation being that the relevant length scale is determined by the sigma mass.

The corresponding thermodynamical potential per volume in the Thomas-Fermi approximation is then

$$\begin{aligned} \omega(\mu) &= \langle \bar{\psi}(\vec{\gamma} \cdot \vec{p})\psi \rangle + g_s \sigma \langle \bar{\psi}\psi \rangle \left( 1 - \frac{G_{sv}}{G_s} \langle \psi^\dagger \psi \rangle^2 \right)^{1/2} \\ &+ g_v V_0 \langle \psi^\dagger \psi \rangle + \frac{1}{2} \vec{\nabla} \sigma \cdot \vec{\nabla} \sigma + \frac{1}{2} m_s^2 \sigma^2 - \frac{1}{2} m_v^2 V_0^2 - \mu \langle \psi^\dagger \psi \rangle \end{aligned} \quad (19)$$

Minimization with respect to  $\sigma$ ,  $V_0$  yields eq. (10) for infinite matter, provided we choose  $G_s = g_s^2/(2m_s^2)$ . Variation with respect to  $M$ ,  $p_F$ ,  $\sigma$  and  $V_0$  gives:

$$\begin{aligned} M &= g_s \sigma \left( 1 - \frac{G_{sv}}{G_s} \langle \psi^\dagger \psi \rangle^2 \right)^{1/2}, \\ E_{p_F} &= \mu - g_v V_0 - g_s \sigma \frac{G_{sv}}{G_s} \langle \bar{\psi}\psi \rangle \langle \psi^\dagger \psi \rangle \left( 1 - \frac{G_{sv}}{G_s} \langle \psi^\dagger \psi \rangle^2 \right)^{-1/2}, \end{aligned}$$



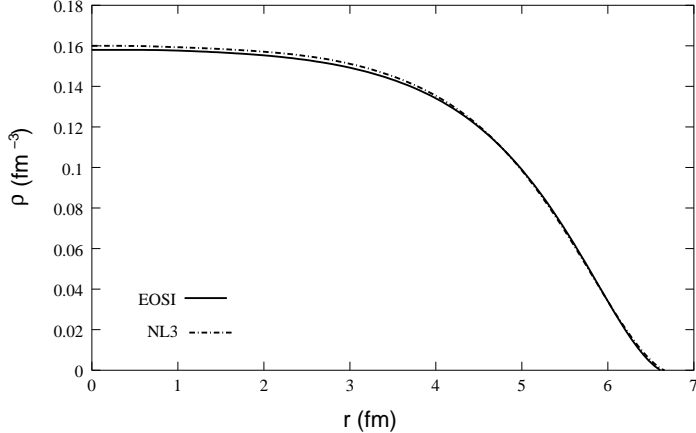


Figure 3: Density profile for nuclei with  $A = 100$

$$\begin{aligned}\nabla^2\sigma &= m_s^2\sigma - g_s\langle\bar{\psi}\psi\rangle\left(1 - \frac{G_{sv}}{G_s}\langle\psi^\dagger\psi\rangle^2\right)^{1/2}, \\ 0 &= m_v V_0 - g_v\langle\psi^\dagger\psi\rangle.\end{aligned}\quad (20)$$

Next, we look for a droplet solution within model I and compare its surface properties with the results obtained with the NL3 parametrization [16]. In the small surface thickness approximation ( $\nabla^2\sigma \sim \frac{d^2\sigma}{dr^2}$ ) the free energy  $F$  can be rewritten as [21]:

$$F = \int 4\pi r^2 dr \left( \left( \frac{d\sigma}{dr} \right)^2 - C \right) + \mu A, \quad (21)$$

where  $C$  is a constant and  $A$  is the number of particles. For droplets with radius  $R$  and volume  $V$ ,

$$F(R) = W_{surf} A^{2/3} - CV + \mu A. \quad (22)$$

The surface energy per unit area of these droplets in the small thickness approximation is

$$W_{surf} = \frac{4\pi R^2}{A^{2/3}} \int_0^\infty dr \left( \frac{d\sigma}{dr} \right)^2. \quad (23)$$

The surface thickness  $t$  is defined as the width of the region where the density drops from  $0.9\rho_{B0}$  to  $0.1\rho_{B0}$ , where  $\rho_{B0}$  is the baryonic density at  $r = 0$ . In Table 2, the values of  $W_{surf}$ ,  $R$ ,  $t$ , for a nucleus with  $A = 100$ , predicted by model I is displayed and compared with the corresponding results obtained by the NL3 parametrization. In the present approach the mass of the  $\sigma$  meson appears as an extra parameter. We have chosen  $m_s = 2m_q = 626$  MeV, as in the NJL model. In Fig. 3 we plot the density profile of a nucleus with 100 particles.

## 5 Isospin asymmetric nuclear matter

The recent advance in unstable nuclear-beam experiments has been providing us with new knowledge on unstable nuclei away from the stability line. We hope to get information on

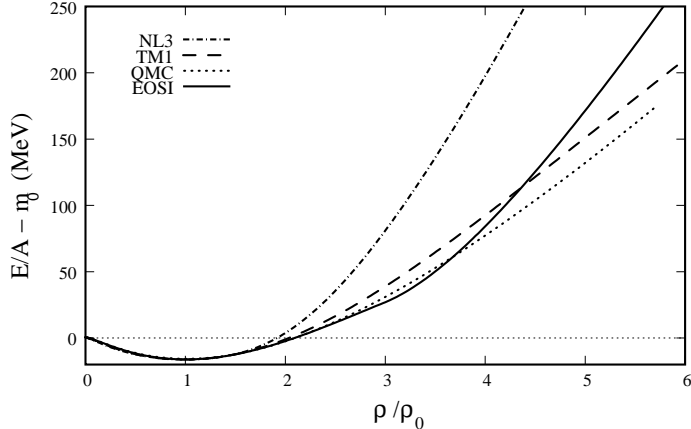


Figure 4: Binding energy versus density according to QMC, EOSI, NL3 and TM1, for symmetric nuclear matter

the properties of dense matter under extreme conditions as the neutron-rich environment in neutron stars.

In order to describe isospin asymmetric nuclear matter within the present formalism it is important to include in the Lagrangian density the isovector-vector term

$$\mathcal{L}_\rho = -G_\rho \left[ (\bar{\psi} \gamma^\mu \vec{\tau} \psi)^2 + (\bar{\psi} \gamma_5 \gamma^\mu \vec{\tau} \psi)^2 \right].$$

Here,  $G_\rho$  is chosen in such a way that the experimental value of the symmetry energy  $a_{sym} = 35$  MeV is reproduced.

In Fig. 4 we compare EOSI with two different parametrizations of the non-linear Walecka model, NL3 [16] and TM1 [22], and the quark meson coupling model (QMC) [14] for symmetric matter. In QMC the structure of nucleons is taken into account having as underlying model the MIT Bag model. In Fig. 5 we make a similar comparison with NL3 and TM1 for neutron matter. The RMF parametrizations were fitted to both stable and unstable nuclei. However TM1 contains a self-coupling term in the vector meson which weakens the contribution of the vector meson at high densities. We conclude that EOSI is softer than NL3. Indeed, EOSI is also softer than TM1 and QMC, but becomes slightly stiffer at higher densities, in connection with chiral symmetry restoration.

The nuclear EOS, as function of density and asymmetry, is reasonably well approximated by:

$$\frac{E}{A} = W = |W_0| \left[ (-2(1 - \delta) \frac{\rho}{\rho_0} + \left(\frac{\rho}{\rho_0}\right)^2 \right] \quad (24)$$

where  $\delta = (\rho_n - \rho_p)/(\rho_n + \rho_p)$ . Here,  $\rho_i$ ,  $i = n, p$  is the density of particles of type  $i$ .

## 6 Original NJL Model in Two Dimensions

For the two dimensional NJL model, we get simple analytic results. The average kinetic energy  $T$  is given by:

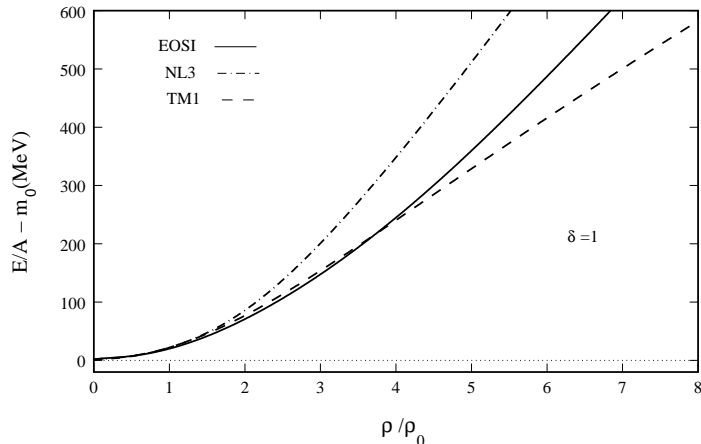


Figure 5: Binding energy versus density according to EOSI, NL3 and TM1, for neutron matter

$T = \frac{1}{2} \rho_f - \frac{1}{6} \rho_f^2 + \dots$ , where  $\rho_f = 2\pi \rho_N$ . Thus we get, ( $c_{sv} = 0$  for pure NJL):

$$m = 1 - g \rho_f - \left(g - \frac{1}{2}\right) \rho_f^2 + \dots, \quad (25)$$

$$W = -\frac{g-1}{2} \rho_f + 0 \rho_f^2 + \dots, \quad (26)$$

where  $g = \frac{\tilde{V}_s}{2\pi}$  and  $m$  is the quark mass. For the two dimensional case, we can obtain exact results for these two quantities, not just for low densities:

$$m^2 = 1 - 2g \rho_f + (g-1)^2 \rho_f^2, \quad (27)$$

$$W = -\frac{g-1}{2} \rho_f. \quad (28)$$

It is remarkable that higher order terms in  $W$ , cancel exactly. The vanishing term of order  $\rho_f^2$  in Eq. (28) has three components which cancel exactly:

1. Relativistic correction to energy momentum relation.
2. Increased kinetic energy due to reduced effective nucleon mass.
3. Increased attraction due to reduction in effective mass of scalar meson (similar to that of the nucleon).

For the more realistic three dimensional case, the physics is very similar, and again there is a near cancellation between these three terms. It cannot, of course, be perfect, since in three dimensions, these terms are proportional to  $\rho^{4/3}$ ,  $\rho^{5/3}$  and  $\rho^2$ , respectively. This explains why the  $c_{sv}$  term is essential for achieving saturation.

## 7 Connection with other Models

### 7.1 Guichon quark meson coupling model

One promising possibility is the quark-meson coupling model proposed by Guichon [14]. In this model, the nucleon mass is generated dynamically using a MIT bag model. Let us

define the dimensional coupling constant:

$$B_s = \frac{g_s^2}{m_s^2} \frac{\rho_0}{M} = \frac{\rho_0 \tilde{V}_s}{M}, \quad (29)$$

where  $\tilde{V}_s$  is the volume integral of the  $NN$  interaction, eq. (6). Then in the Guichon model, we automatically obtain a saturating term which can be put into our form:

$$W_{\rho^2} = c_{sv} B_s^2 \hat{\rho}^2 M c^2 \quad (30)$$

where  $c_{sv} = 0.340 \frac{m_q c}{\hbar} r_{bag}$ , and  $\hat{\rho} = \frac{\rho}{\rho_0}$ . The coefficient 0.340 is a dimensionless constant which can be derived from the MIT bag model [14]. In that work, nuclear matter saturation and some properties of finite nuclei are fitted with a bag radius of  $r_{bag} = 0.8 fm$ . This means that:  $c_{sv} = 0.340 \cdot \frac{313}{197} \cdot 0.8 = 0.432$ , essentially the same as 0.427 obtained using the ENJL model. Their value for the volume integral of the scalar coupling is  $\tilde{V}_s = -1719 MeV fm^3$ , very close to the ENJL result,  $\tilde{V}_s = -1705 MeV fm^3$ .

## 7.2 Relativistic Mean Field Models for Equation of State

In the non-linear and derivative coupling mean field models, we also get a term quadratic in the density. In the strong coupling limit, neglecting kinetic energy, we can write for the energy per particle:

$$W = M - 1 + \frac{1}{2} B_v \hat{\rho} + \frac{(M - 1)^2}{2 B_s \hat{\rho} M^\alpha} \quad (31)$$

The effective mass is obtained by setting  $\frac{dW}{dM} = 0$ .

In the low density limit, the effective mass is given by:

$$M = 1 - B_s \hat{\rho} + \frac{3}{2} \alpha B_s^2 \hat{\rho}^2 + \dots \quad (32)$$

and

$$W = \frac{1}{2} (B_v - B_s) \hat{\rho} + \frac{1}{2} \alpha B_s^2 \hat{\rho}^2 + \dots \quad (33)$$

Making a comparison with Eq. (30), we obtain  $c_{sv} = \frac{1}{2} \alpha$ . In the original derivative coupling model [23], we get  $\alpha = 2$ , and  $c_{sv} = 1$ , which seems too large. However, in the hybrid model developed by Glendenning *et al* [24], we have  $\alpha = 1$ , which corresponds to  $c_{sv} = 0.5$ . This is close to our phenomenological result. On the other hand, with the other EOS parametrizations,  $c_{sv}$  has different values.

## 7.3 Connection of ECS model to other relativistic chiral models

In the present form the Lagrangian density (14) contains terms coupling the meson fields to the fermion fields in a non-linear way. Using the equations of motion and keeping only quartic terms in the meson fields we get,

$$\begin{aligned} \mathcal{L} &= \bar{\psi}(i\gamma^\mu \partial_\mu)\psi - g_s (\sigma \bar{\psi}\psi + \bar{\psi}i\gamma_5 \vec{\pi} \cdot \vec{\tau}\psi) - g_v \bar{\psi}V^\mu \gamma_\mu \psi \\ &+ \frac{1}{2}(\partial^\mu \sigma \partial_\mu \sigma + \partial^\mu \vec{\pi} \cdot \partial_\mu \vec{\pi}) - \frac{1}{2}m_s^2(\sigma^2 + \vec{\pi} \cdot \vec{\pi}) - \frac{1}{4}V^{\mu\nu}V_{\mu\nu} + \frac{1}{2}m_v^2 V^\mu V_\mu \\ &+ \frac{1}{2} \frac{g_s m_v^4}{g_v^2} a_1 (\sigma^2 + \vec{\pi} \cdot \vec{\pi}) V^\mu V_\mu. \end{aligned} \quad (34)$$

This Lagrangian density, except for the meson kinetic terms, is similar to the one introduced by Boguta [5] which, by including a scalar-vector coupling, was able to reproduce nuclear matter saturation properties. However, in [5] an effective mesonic self-interaction corresponding to the “Mexican hat” is present.

In [6] a generalization of the model proposed in [5], including a “bare” vector mass, a quartic term in vector field and allowing for different vector-scalar and vector-nucleon couplings, was studied. It was argued that a linear realization of chiral symmetry was too restrictive and, although nuclear matter properties may be reproduced, there are problems with the properties of finite nuclei. In our formulation, however, and with our choice of parameters we have shown that not only nuclear matter saturation properties are reasonably explained, but also surface properties.

## 8 Conclusions

We have studied an extension of the NJL model which yields reasonable saturation of nuclear matter. An effective density dependent coupling constant is obtained which pushes chiral symmetry restoration to higher densities. Two variants of the model defined by appropriate sets of the parameters,  $G_s$ ,  $G_v$ ,  $G_{sv}$ , and  $\Lambda$ , have been studied numerically. For Model I, the values of the defining parameters, the vacuum properties, the properties at saturation are given in Tables 1 and 2. An extension of the chiral sigma model has been developed which is based on the extended NJL model and fits not only the properties at saturation but also the empirical nuclear surface energy and thickness. The term in  $G_{sv}$ , responsible for the density dependence of the effective coupling constant, plays an important role in pushing to higher densities the restoration of chiral symmetry and in lowering the incompressibility.

The relation of the present model to the relativistic chiral model proposed by Boguta [5] was presented. Finally we have discussed asymmetric matter within the present model.

We have shown the connection of the ENJL model with other relativistic models including QMC, ECS, non-linear and derivative coupling mean field models. In order to further test the model it is important to calculate other properties of finite nuclei and its performance at finite temperature. The critical temperature for chiral symmetry restoration at zero density is easily calculated to be  $T_c = 196$  MeV, an encouraging result. Application of the model to neutron-star matter requires the inclusion of strangeness and beta-equilibrium.

## Acknowledgments

The authors would like to thank Mitja Rosina for fruitful discussions. This work was partially supported by FCT and FEDER under the projects POCTI/FIS/451/94, POCTI/35308/FIS/2000, and POCTI/FP/FNU/50326/2003.

## References

- [1] Y. Nambu and G. Jona-Lasinio, Phys. Rev. **122**, 345 (1961); **124**, 246 (1961).

- [2] U. Vogl and W. Weise, *Prog. Part. and Nucl. Phys.* **27**, 95 (1991).
- [3] S. P. Klevansky, *Revs. of Mod. Physics* **64**, 649 (1992).
- [4] T. Hatsuda and T. Kunihiro, *Prog. Theo. Phys.* **74**, 765 (1985); T. Hatsuda and T. Kunihiro, *Phys. Rep.* **247**, 221 (1994).
- [5] J. Boguta, *Phys. Lett.* **B 120**, 34 (1983).
- [6] R. J. Furnstahl and B. D. Serot, *Phys. Rev.* **C47**, 2338 (1993).
- [7] V. Koch, T.S. Biro, J. Kunz, and U. Mosel, *Phys. Lett.* **B 185**, 1 (1987).
- [8] W. Bentz and A.W. Thomas, *Nucl. Phys.* **A 696**, 138 (2001).
- [9] C. Providência, João da Providência and S. Moszkowski, in “*Proc. of the 11th Int. Conf. on Recent Progress in Many-Body Theories*”, R. F. Bishop, K. A. Gernoth, N. R. Walet and Y. Xian (Eds) (World Sci. Singapore, 2002) 242; C. Providência, J. M. Moreira, J. da Providência and S. A. Moszkowski, in “*Hadron Physics: Effective theories of low energy QCD*”, A. Blin, B. Hiller, M. C. Ruivo, E. van Beveren (eds.), AIP Conf. Proc. vol. 660 (New York, 2003) 231.
- [10] I. N. Mishustin, L. M. Satarov and W. Greiner, *Physics Repts.* **391**, 363 (2004)
- [11] T.J. Burvenich, and D.G. Madland, *Nucl. Phys.* **A 729**, 769 (2003).
- [12] H. Bohr, C. Providencia, and J. da Providencia, *Phys. Rev.* **C 71**, 055203 (2005)
- [13] A.H. Rezaeian and H.-J. Pirner, nucl-th/0510041
- [14] P.A.M. Guichon, *Phys. Lett.* **B 200**, 235, (1988), P.A.M. Guichon, K. Saito, E. Rodionov, and A.W. Thomas, *Nucl. Phys.* **A 601**, 349, (1996).
- [15] R. J. Furnstahl, Brian D. Serot, Hua-Bin Tang, *Nucl. Phys.* **A 615**, 441 (1997).
- [16] G.A. Lalazissis, J. König, P. Ring, *Phys. Rev.* **C55**, 540 (1997).
- [17] T.D.Lee, *Particle Physics and Introduction to Field Theory*, Harwood, Acad. Publ. London, (1981).
- [18] M. Fiolhais, J. da Providencia, M. Rosina, and C. A. de Sousa, *Phys. Rev.* **C56**, 3311 (1997)
- [19] J. Providencia, H. Walliser, H. Weigel, *Nucl.Phys.* **A 671**, 547 (2000); M. Centelles, X. Viñas, M. Barranco, and P. Schuck, *Ann. Phys. (NY)* **221**, 165 (1993)
- [20] H. Reinhardt, *Phys. Lett.* **B188**, 263 (1987).
- [21] M. Nielsen and J. da Providencia, *J.Phys.* **G 16**, 649 (1990).
- [22] K. Sumiyoshi, H. Kuwabara, H. Toki, *Nucl. Phys.* **A 581**, 725 (1995).
- [23] J. Zimanyi and S. A. Moszkowski, *Phys. Rev.* **C 42**, 1416 (1990).
- [24] N. K. Glendenning, F. Weber and S. A. Moszkowski, *Phys. Rev.* **C 45**, 844 (1992).